

# Insight into the realistic behaviours of magnetic pulse forming and welding processes using numerical simulations

T. Sapanathan<sup>1</sup>, K. Yang<sup>1</sup>, N. Buiron<sup>1</sup> and M. Rachik<sup>1</sup>

<sup>1</sup>*Sorbonne universités, Université de technologie de Compiègne, CNRS, laboratoire Roberval, UMR – 7337, Centre de recherche Royallieu, CS 60 319, 60 203 Compiègne cedex*

# Introduction: Project COILTIM

- Produce efficient welding of similar / dissimilar metal pairs
- Joint quality analysis with process parameters
- Joint quality analysis of the effect of metal dissimilarity
- Modeling and simulation of the MPF/MPW
- Feasibility study and development of processing tools



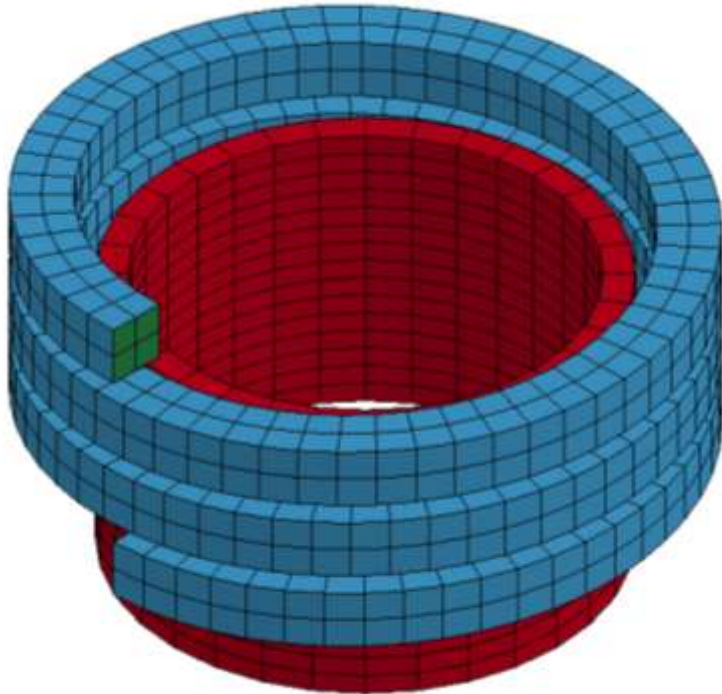
[MPF/MPW: Magnetic Pulse Forming / Magnetic Pulse Welding]

# Outline

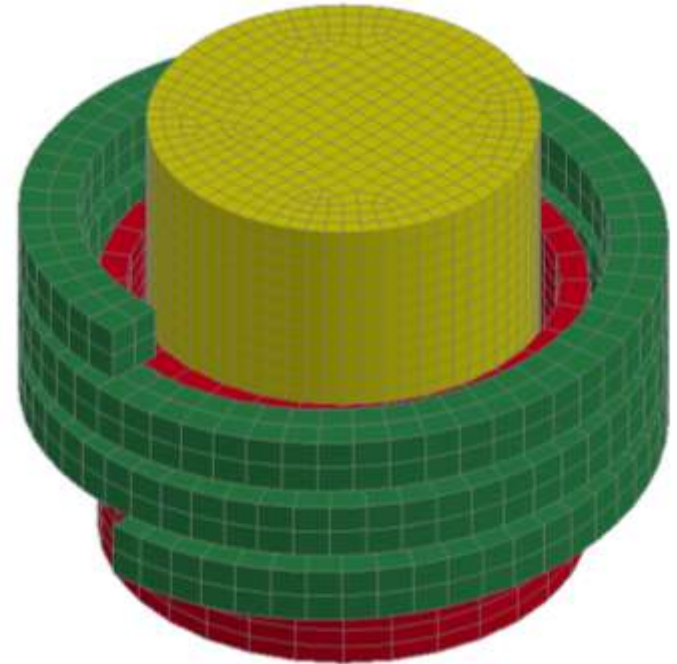
- Methods about the EM numerical modelling, investigating the influence of the cylindrical rod in a MPW
- Main focuses on the numerical modelling of MPW
  - *EM component*
  - *Interfacial behaviour*
  - *Contact behaviour*
- Field shaper effect in forming and welding
- Change in force direction, during MPF/MPW
- Development of negative velocity and spring back effect in ring expansion process
- Identification of material models for MPF/MPW processes

[EM: Electromagnetic; MPF: Magnetic Pulse Forming; MPW: Magnetic Pulse Welding ]

# Preliminary models: Tube compression with and without rod using helix coils

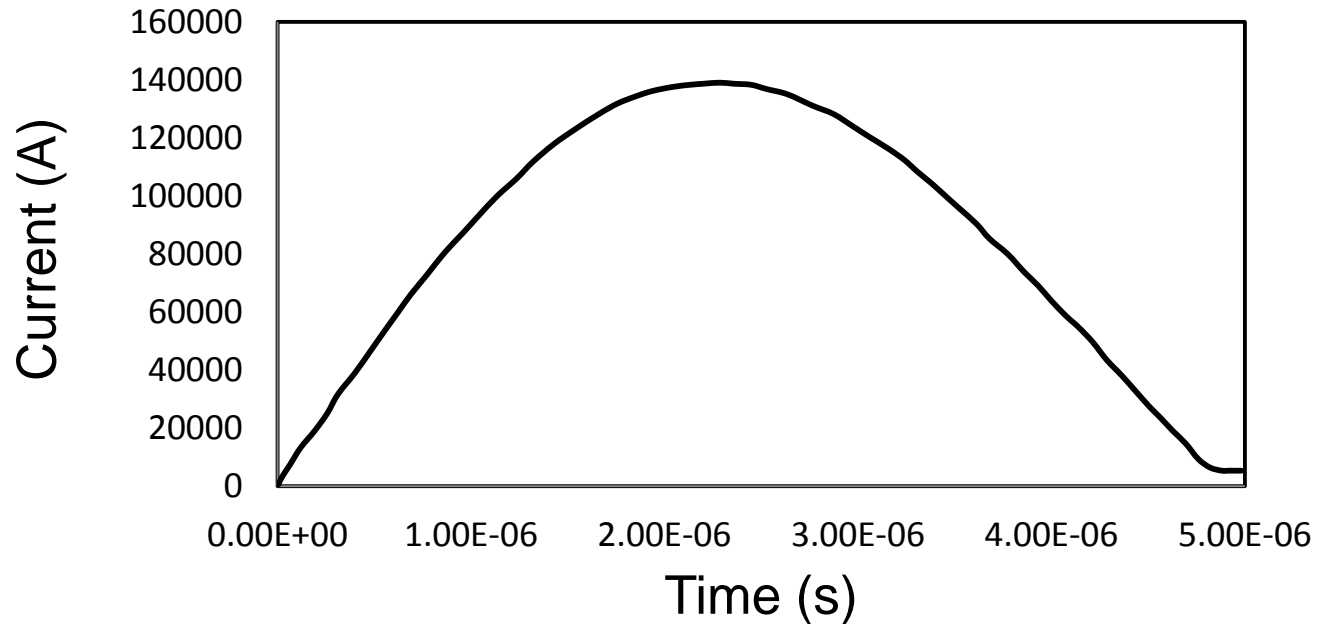


Tube without cylinder rod model



Tube with cylinder rod model

# Input current used in those preliminary models



(I. Henchi et al, 10<sup>th</sup> International LS-Dyna User Conference)

# Material Model

**Table 1**

Johnson–Cook parameter values used to simulate the behaviour of A2024-T351 [17]

| A   | B   | N    | C      | m |
|-----|-----|------|--------|---|
| 352 | 440 | 0.42 | 0.0083 | 1 |

**Table 2**

Workpiece and tool physical parameters [18]

| Physical parameter                                       | Workpiece (A2024-T351)  | Tool (tungsten carbide insert) |
|--|---|--------------------------------|
| Density, $\rho$ (kg/m <sup>3</sup> )                     | 2700  | 11900                          |
| Elastic modulus, $E$ (GPa)                               | 73  | 534                            |
| Poisson's ratio, $\nu$                                   | 0.33  | 0.22                           |
| Specific heat, $C_p$ (J/kg/°C)                           | $C_p = 0.557T + 877.6$  | 400                            |
| Thermal conductivity, $\lambda$ (W/m/C)                  | $25 \leq T \leq 300$ :<br>$\lambda = 0.247T + 114.4$<br>$300 \leq T \leq T_{\text{melt}}$ :<br>$\lambda = 0.125T + 226.0$ | 50                             |
| Expansion, $\alpha_d$ ( $\mu\text{m.m}/^\circ\text{C}$ ) | $\alpha_d = 8.9 \times 10^{-3}T + 22.2$   | ×                              |
| $T_{\text{melt}}$ (°C)                                   | 520   | ×                              |
| $T_{\text{room}}$ (°C)                                   | 25  | 25                             |

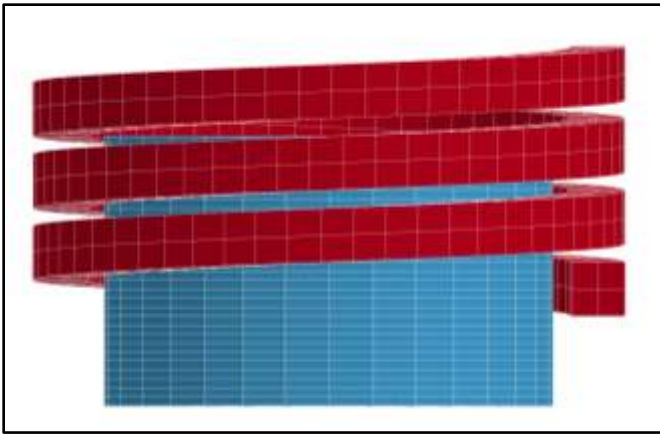
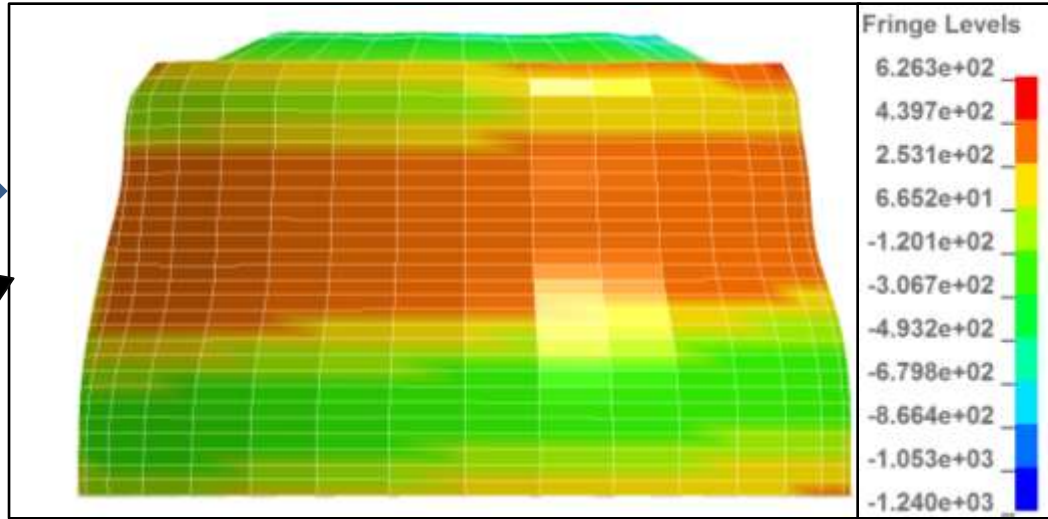
(T. Mabrouki et al. 2008, Int. Journal of Machine tools & Manufacture)

# Electromagnetic properties of material

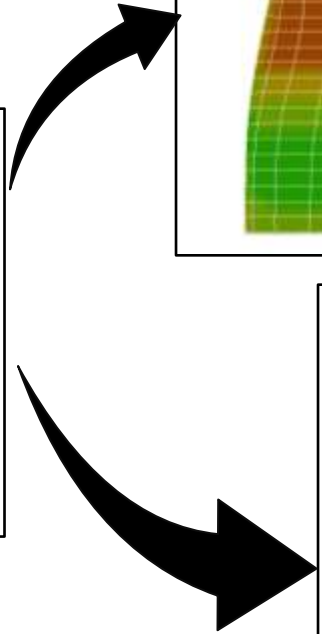
- $\sigma$  of the work piece: Aluminum alloy – 30% IACS ( $1.74 \times 10^4$  S/mm)
- Copper helix coil – 70% IACS ( $4.06 \times 10^4$  S/mm)
- Steel coil – 7% IACS ( $4.06 \times 10^3$  S/mm)
- $\mu_r = \mu / \mu_0$ , for copper alloy, steel and air are considered to be  $\sim 1$
- However this  $\mu_r$  may significantly vary with the type of steel

# Coil geometry and non axisymmetric deformation

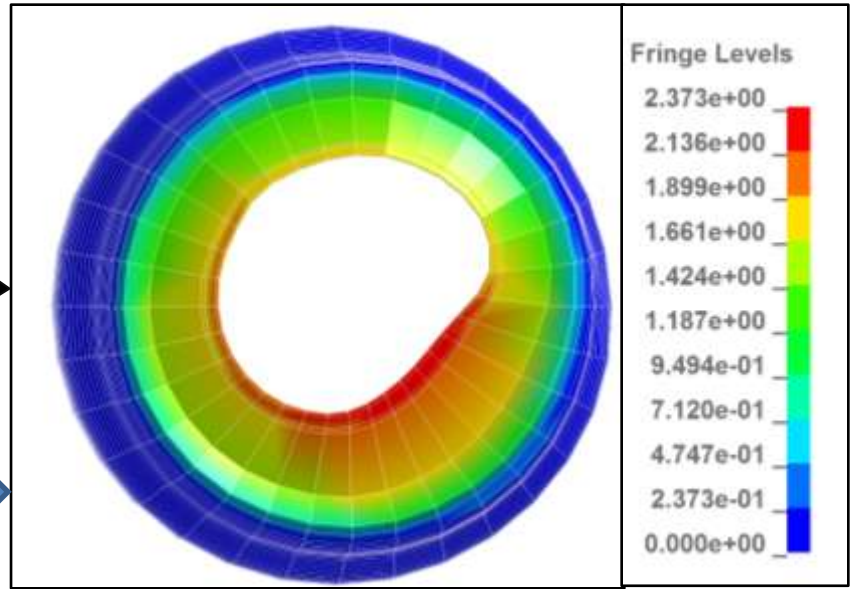
Pressure distribution



Model Geometry

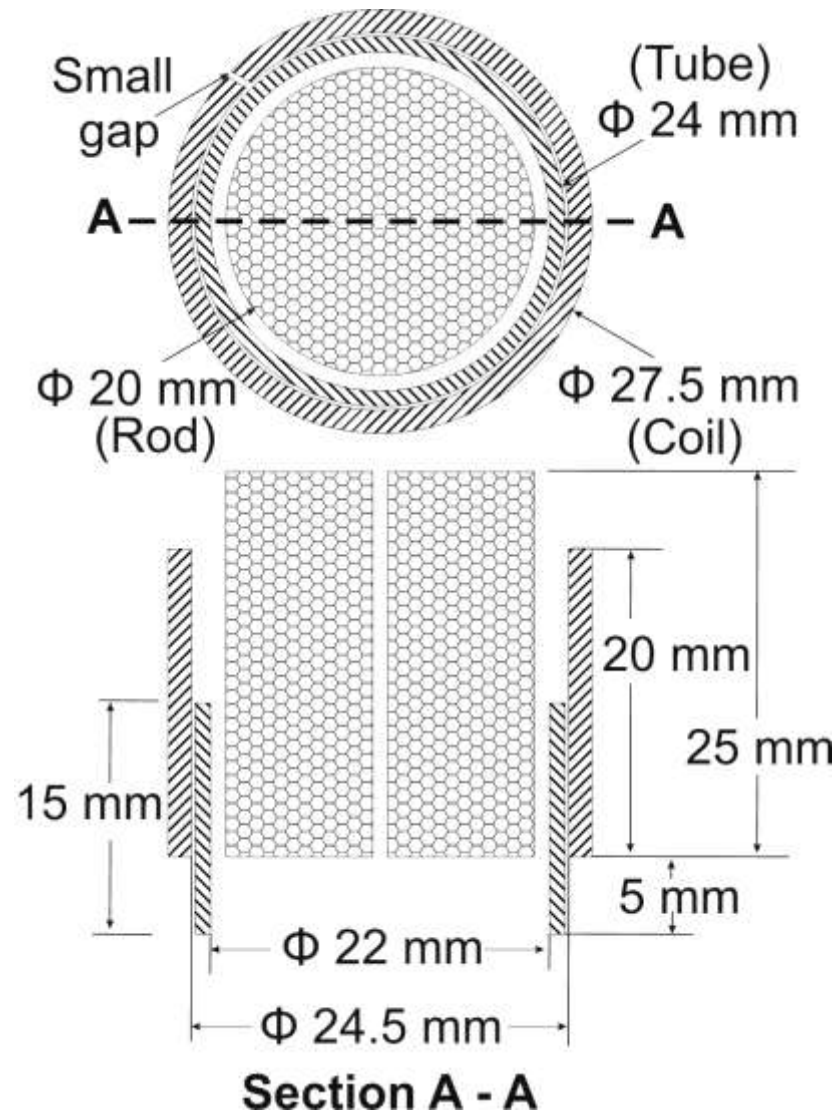


Effective plastic strain distribution



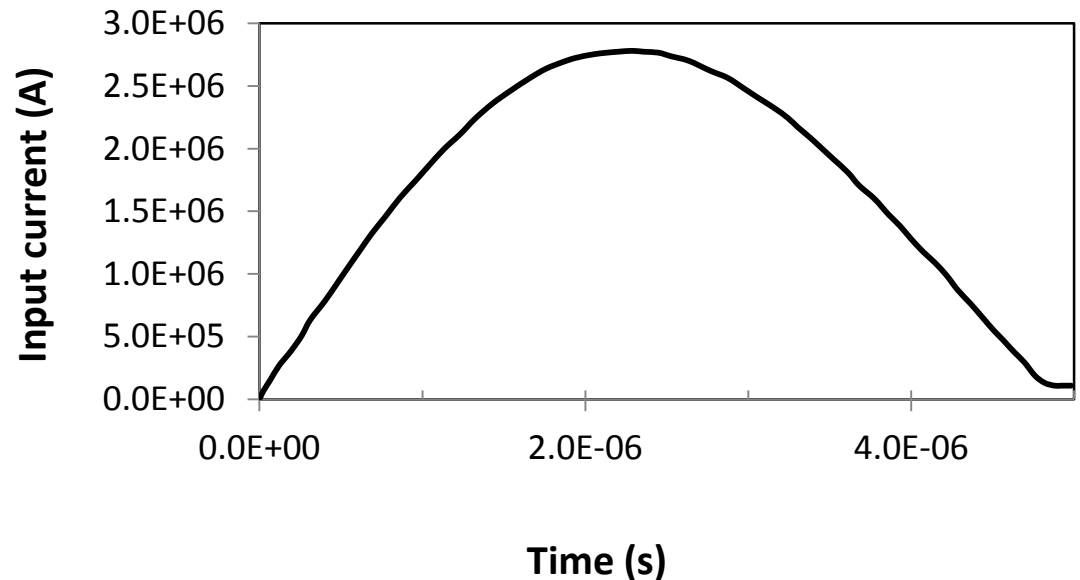
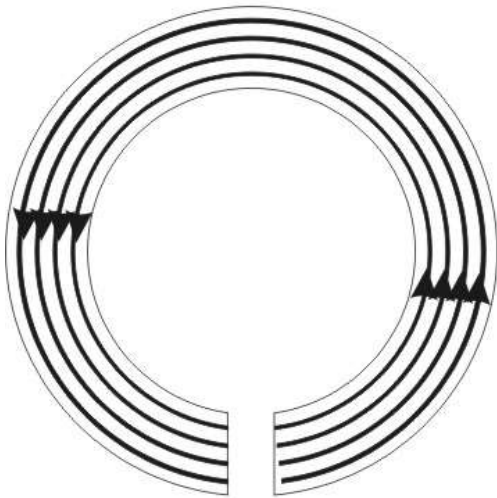


# Model with one turn symmetric coil



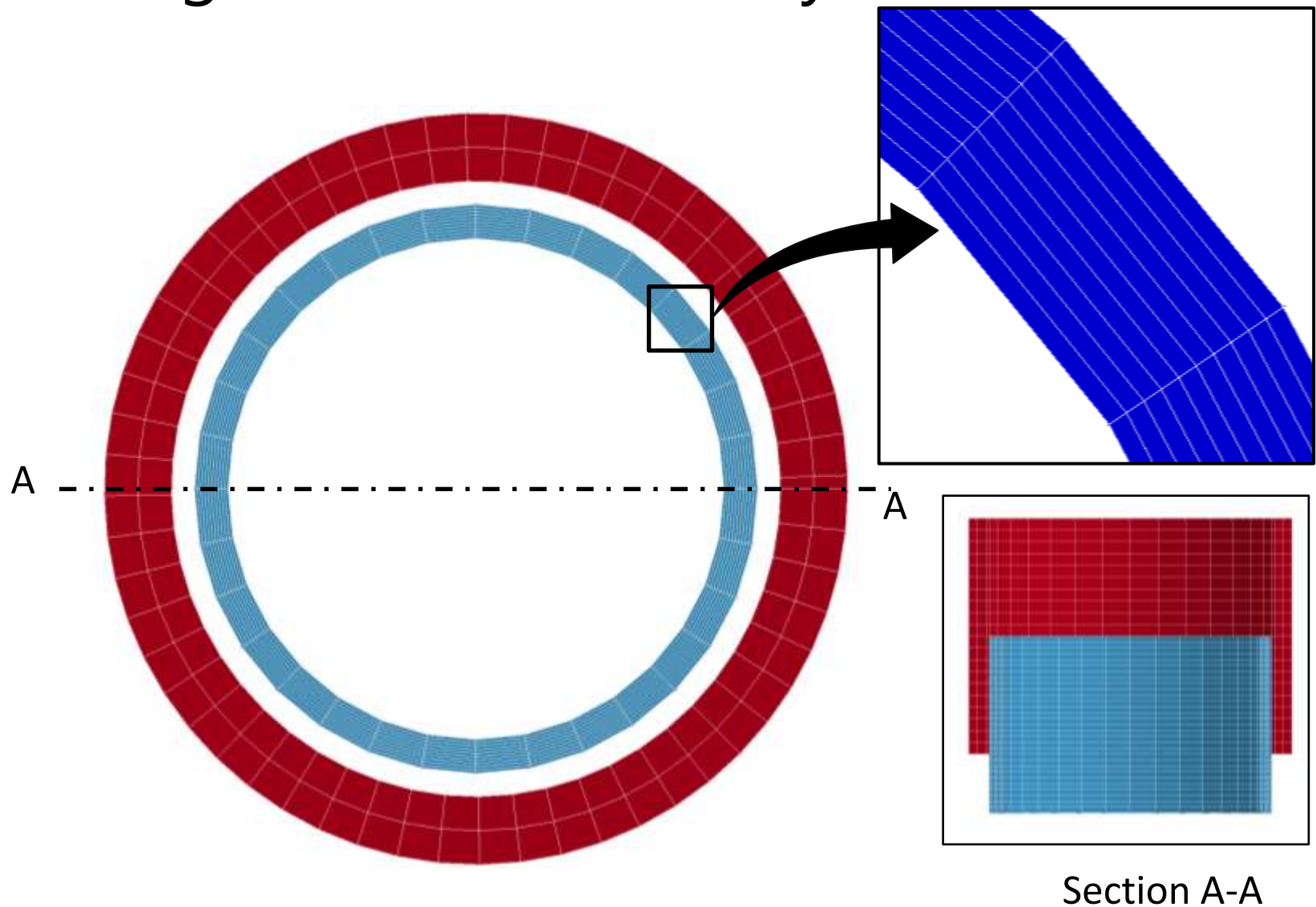
# Material and other parameters

- Core and solid made from aluminium A2024 – T351
- One turn coil with axis-symmetric geometry used and a symmetric current flow expected

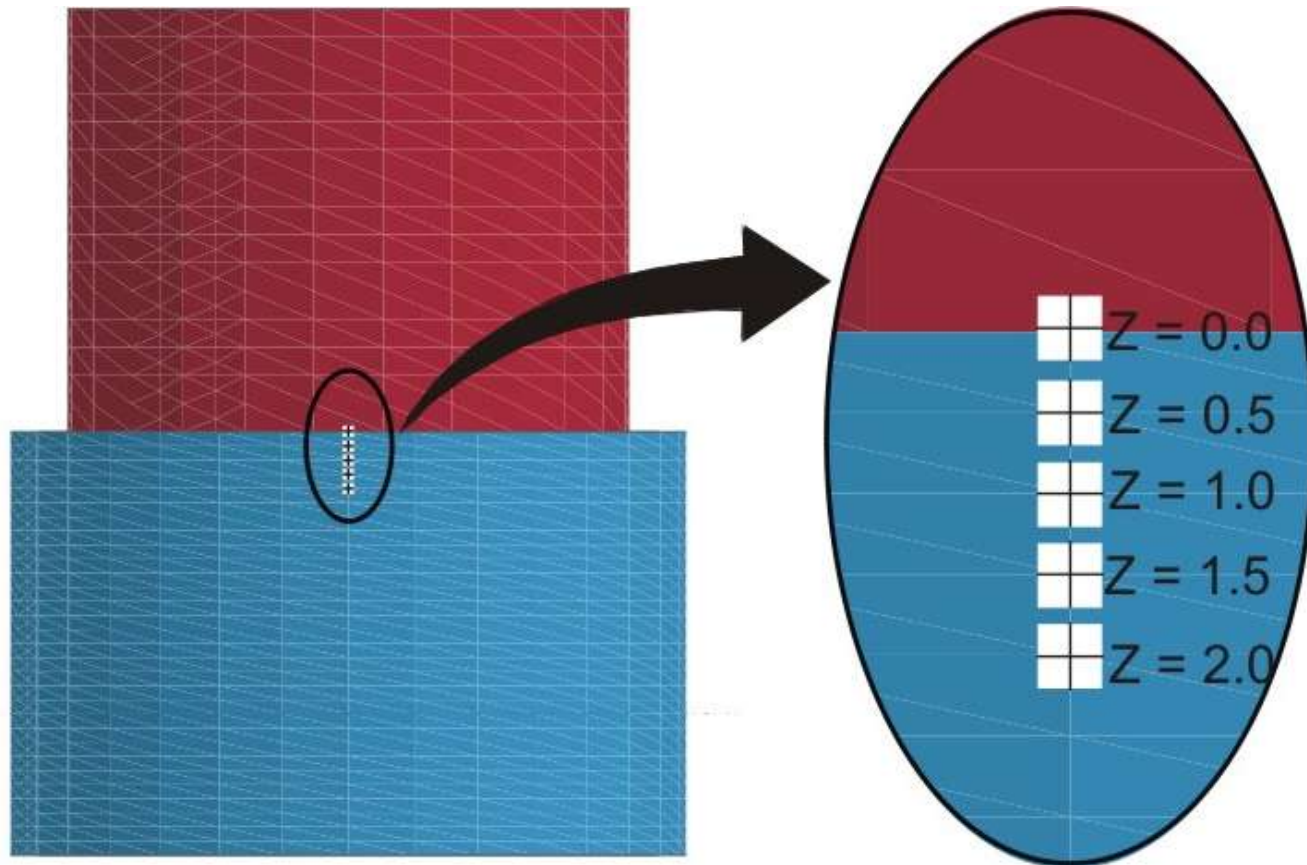


Expected a symmetric current flow

# The multi-layered mesh to capture the gradient of the eddy current



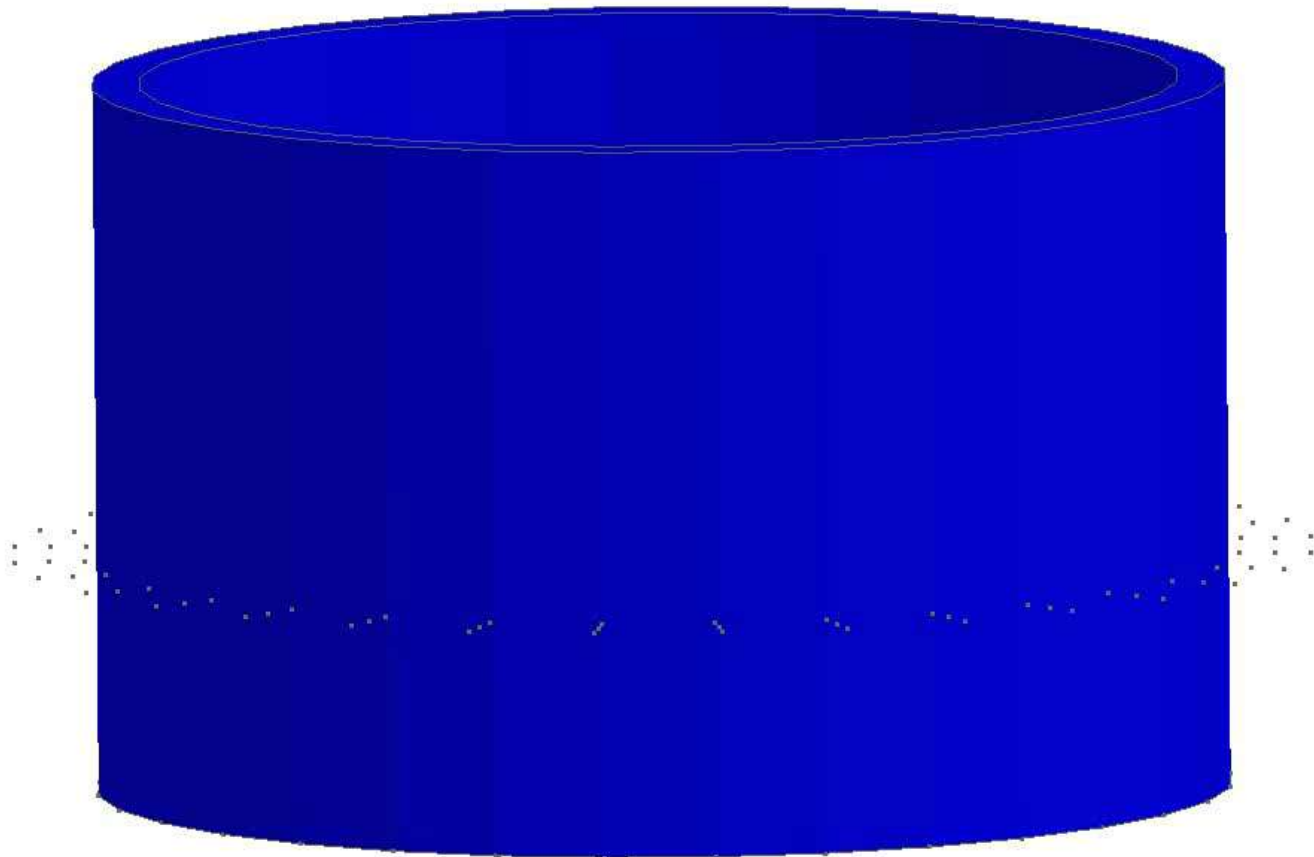
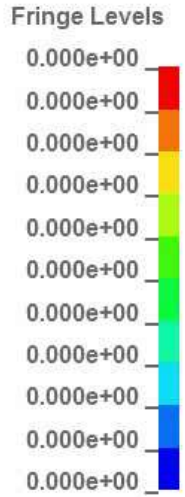
# Investigation of nodal velocity



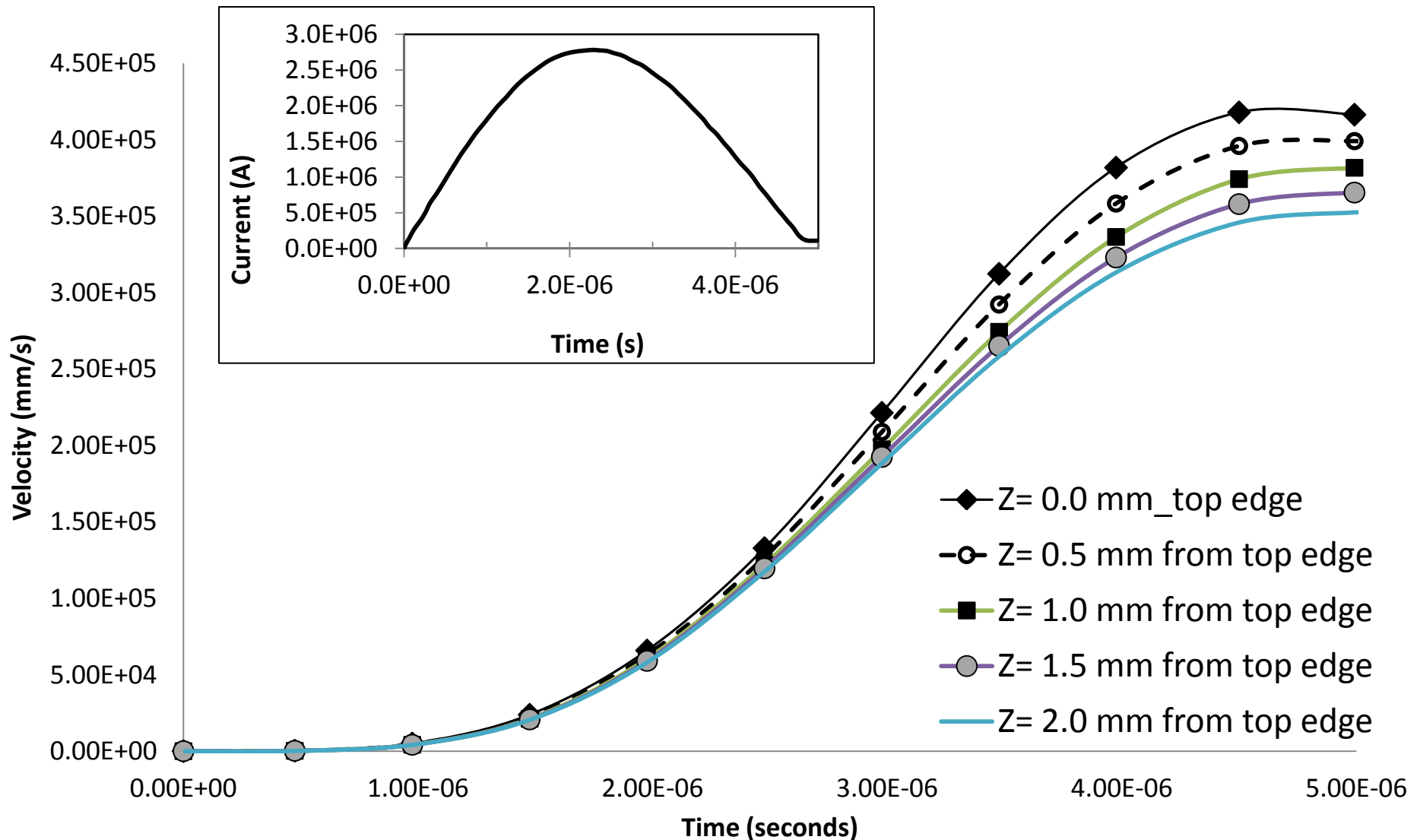
# Model without the cylinder rod

LS-DYNA keyword deck by LS-PrePost

Contours of Effective Plastic Strain  
min=0, at elem# 225  
max=0, at elem# 225



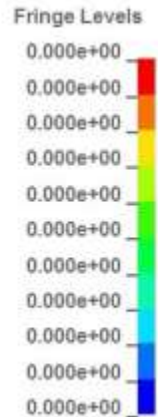
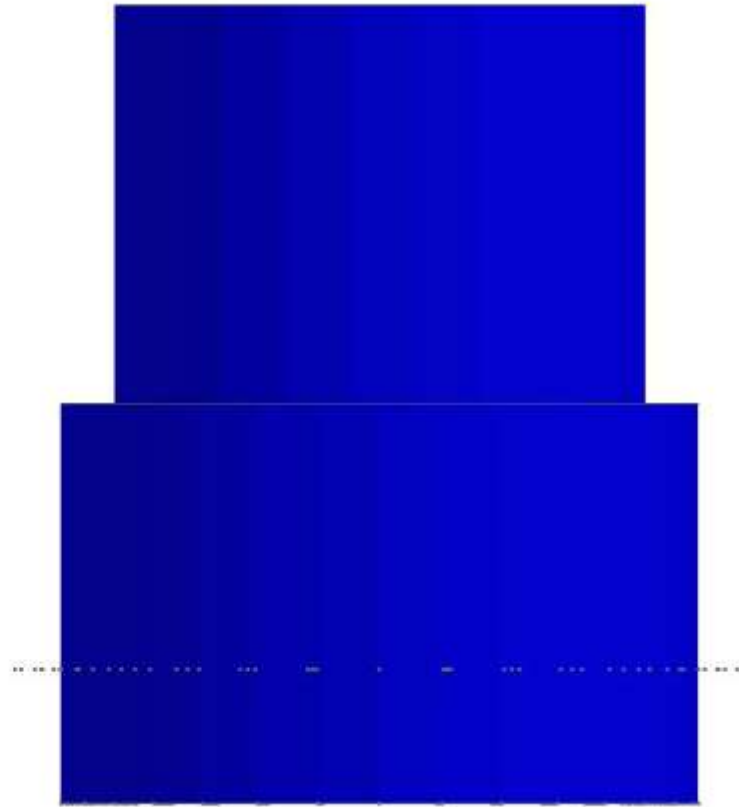
# Nodal velocity from the top edge



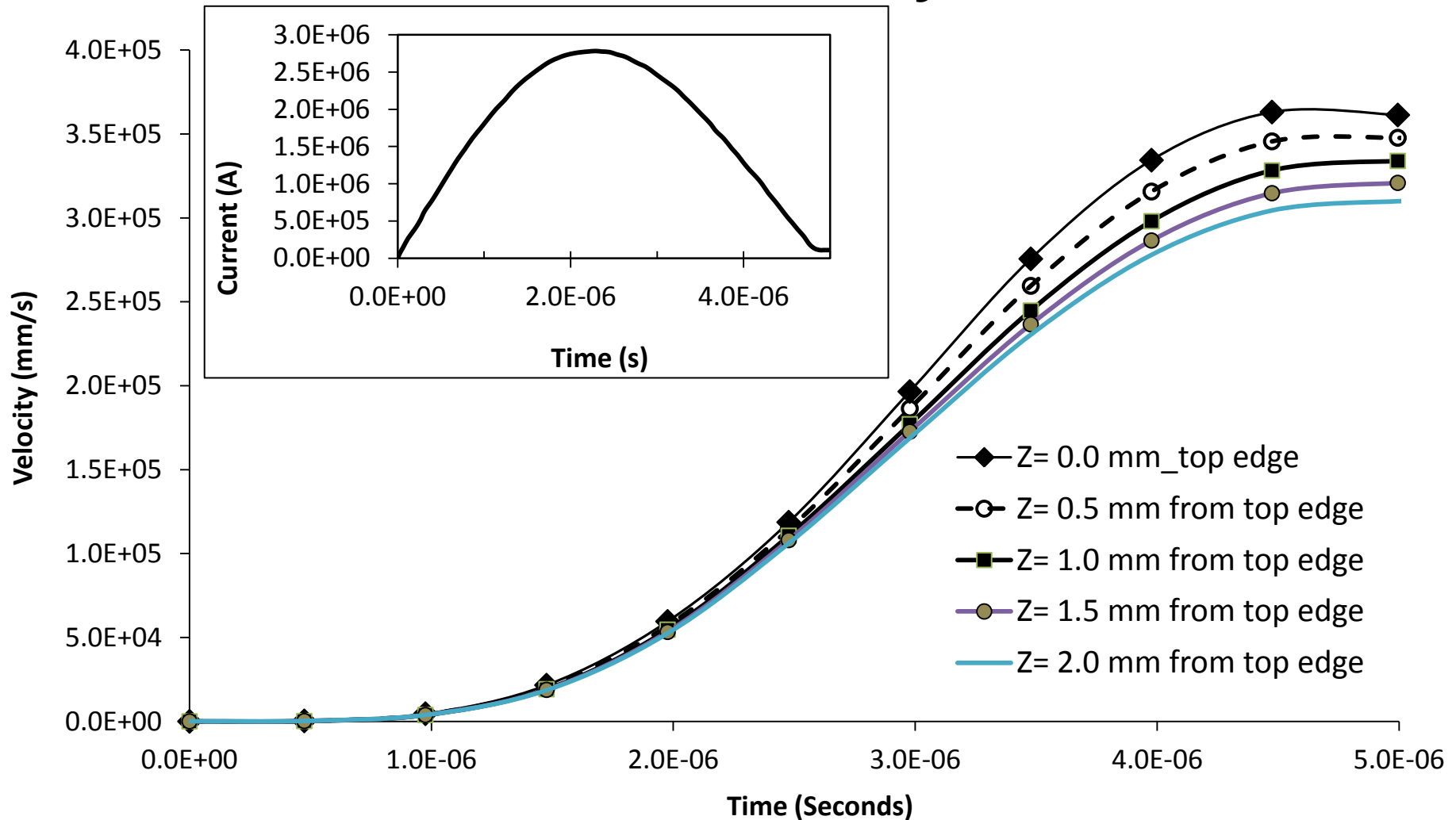
# With Solid rod in the model, but without contact

LS-DYNA keyword deck by LS-PrePost

Contours of Effective Plastic Strain  
min=0, at elem# 225  
max=0, at elem# 225



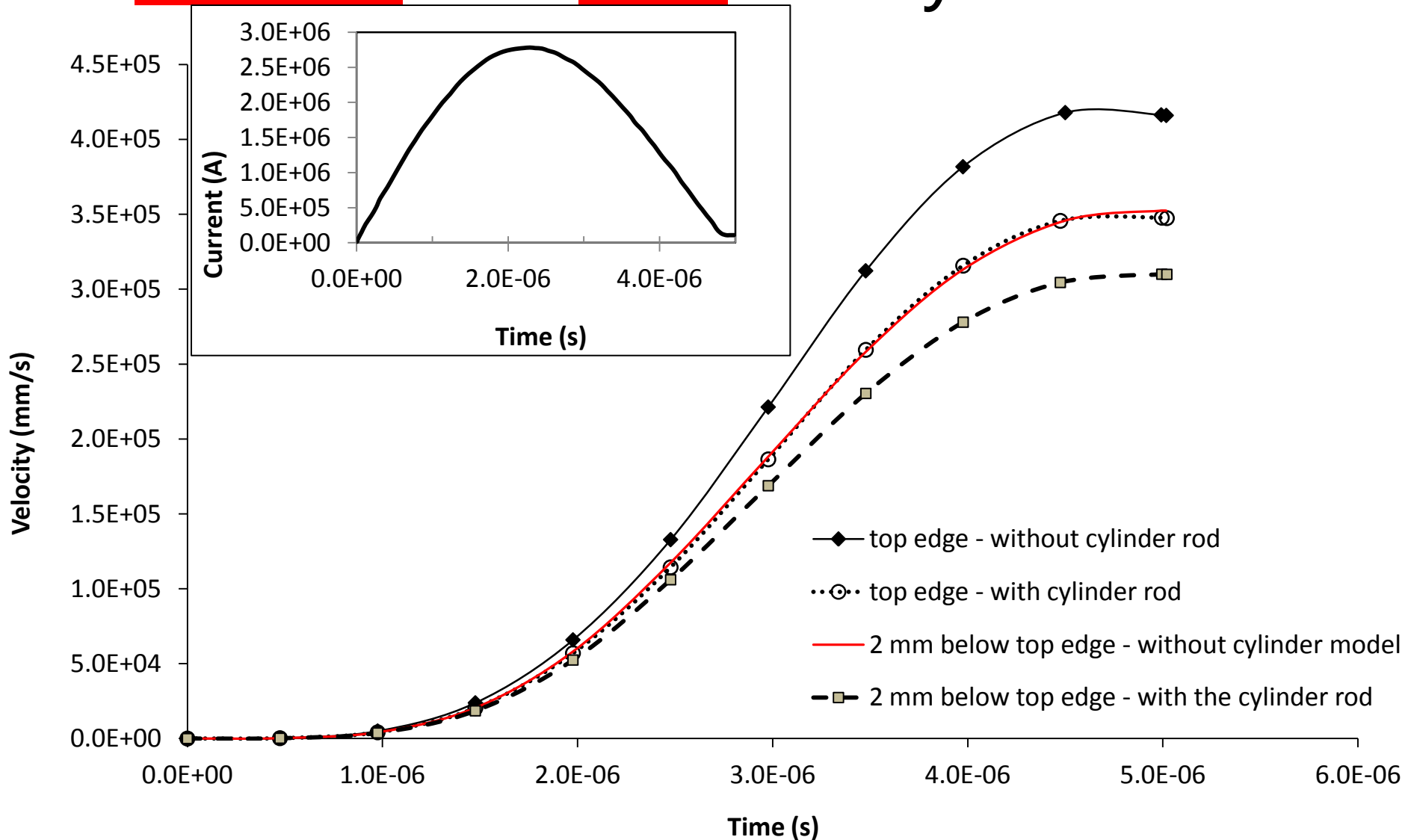
# Nodal velocity from top edge for the model with the cylinder rod



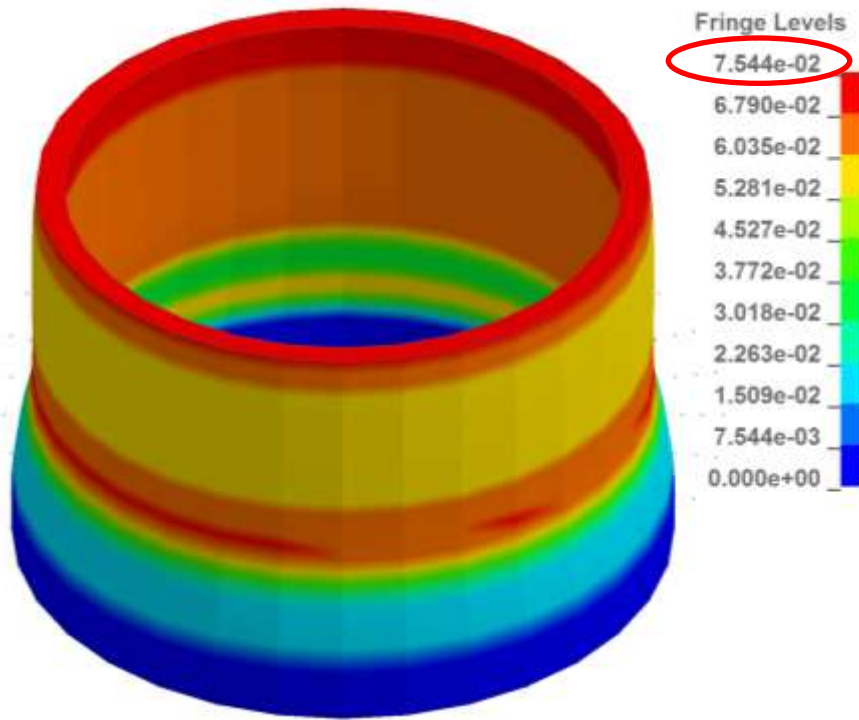


# Comparison of velocity

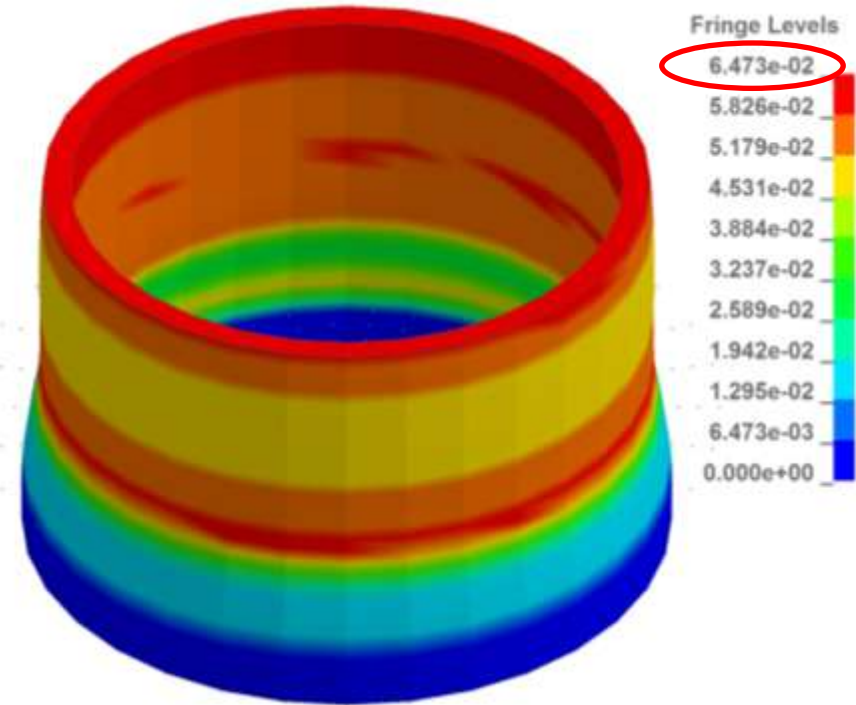
without and with the cylinder rod



# Comparison of plastic strain without and with the cylinder rod



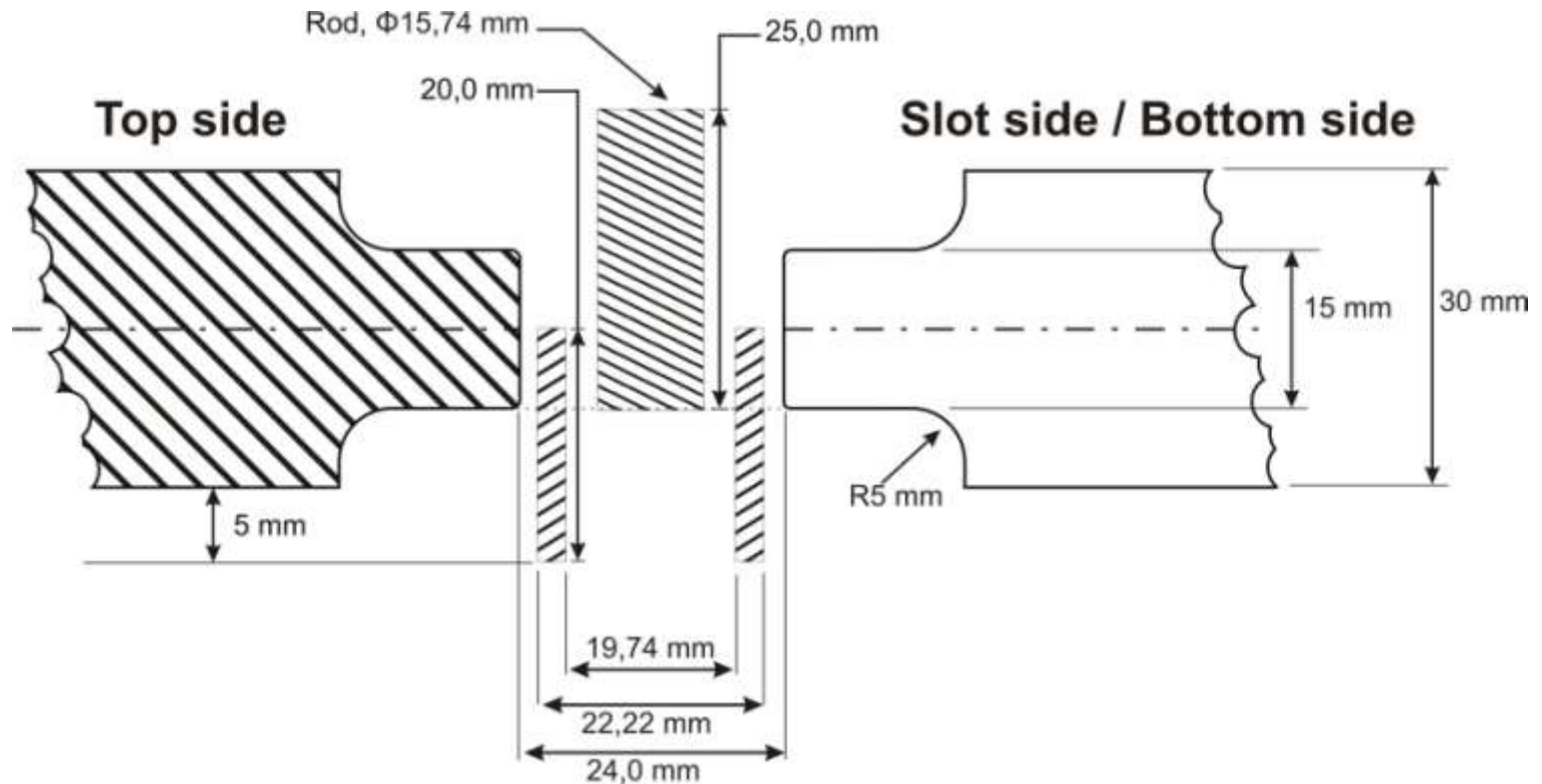
Plastic strain without the cylinder rod  
Maximum : 7.54%



Plastic strain with the cylinder rod  
Maximum: 6.47%

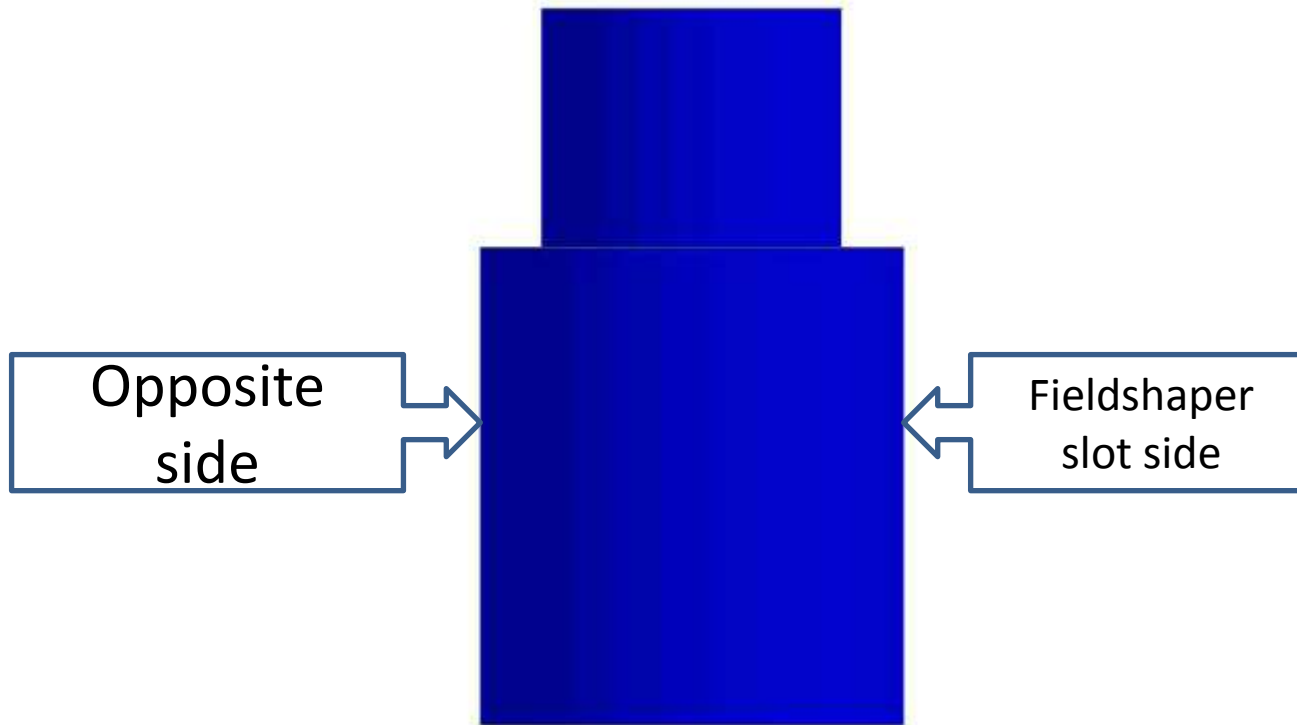
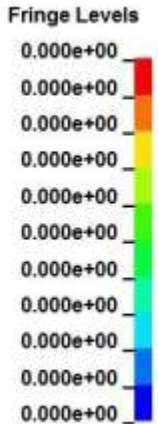
# Welding and contact models

- Mechanical + Electromagnetic contact algorithms used in these models

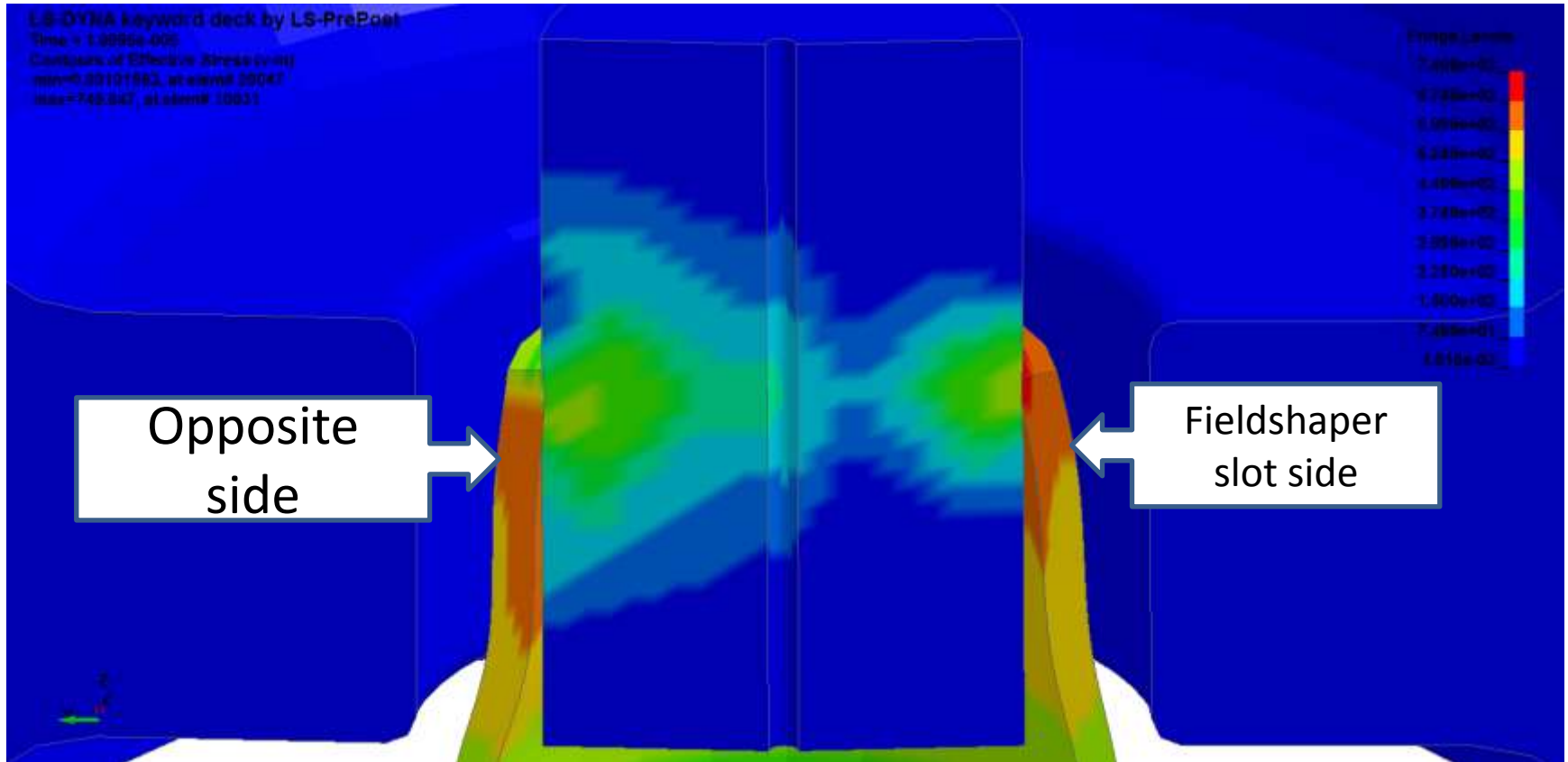


# von Mises stress distribution (MPa)

LS-DYNA keyword deck by LS-PrePost  
Time = 0  
Contours of Effective Stress (v-m)  
min=0, at elem# 251  
max=0, at elem# 251



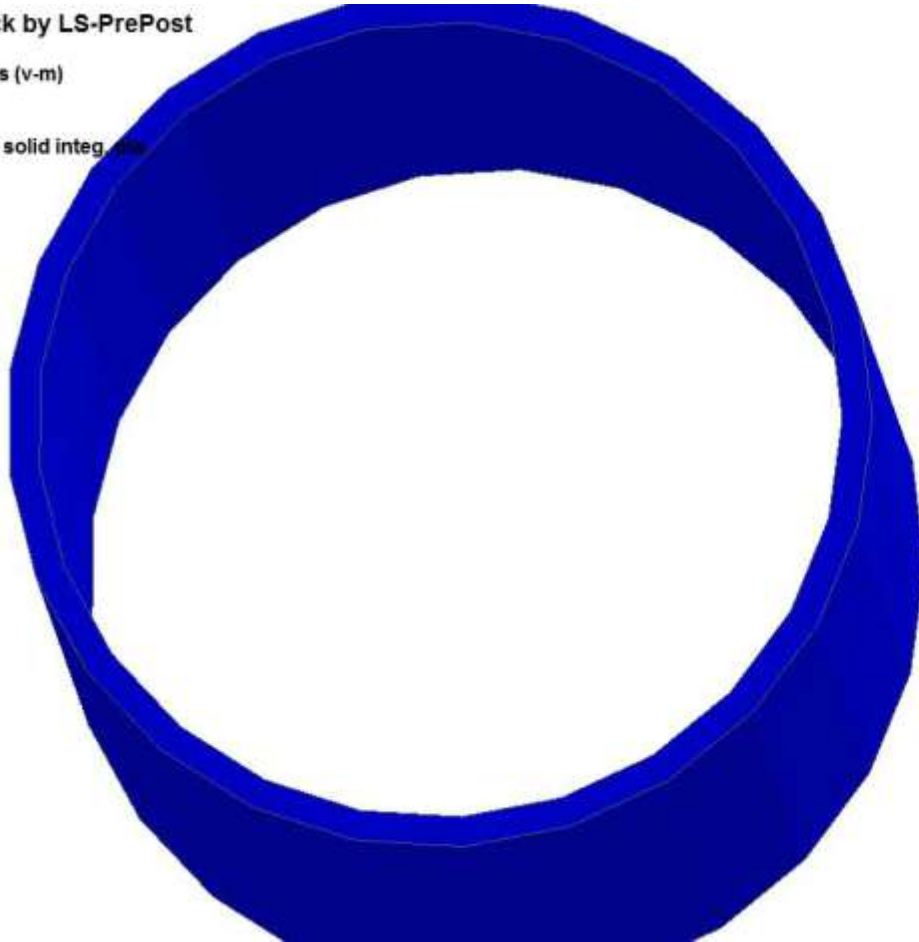
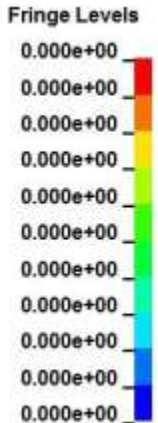
# Effective stress at the beginning of the impact (MPa)



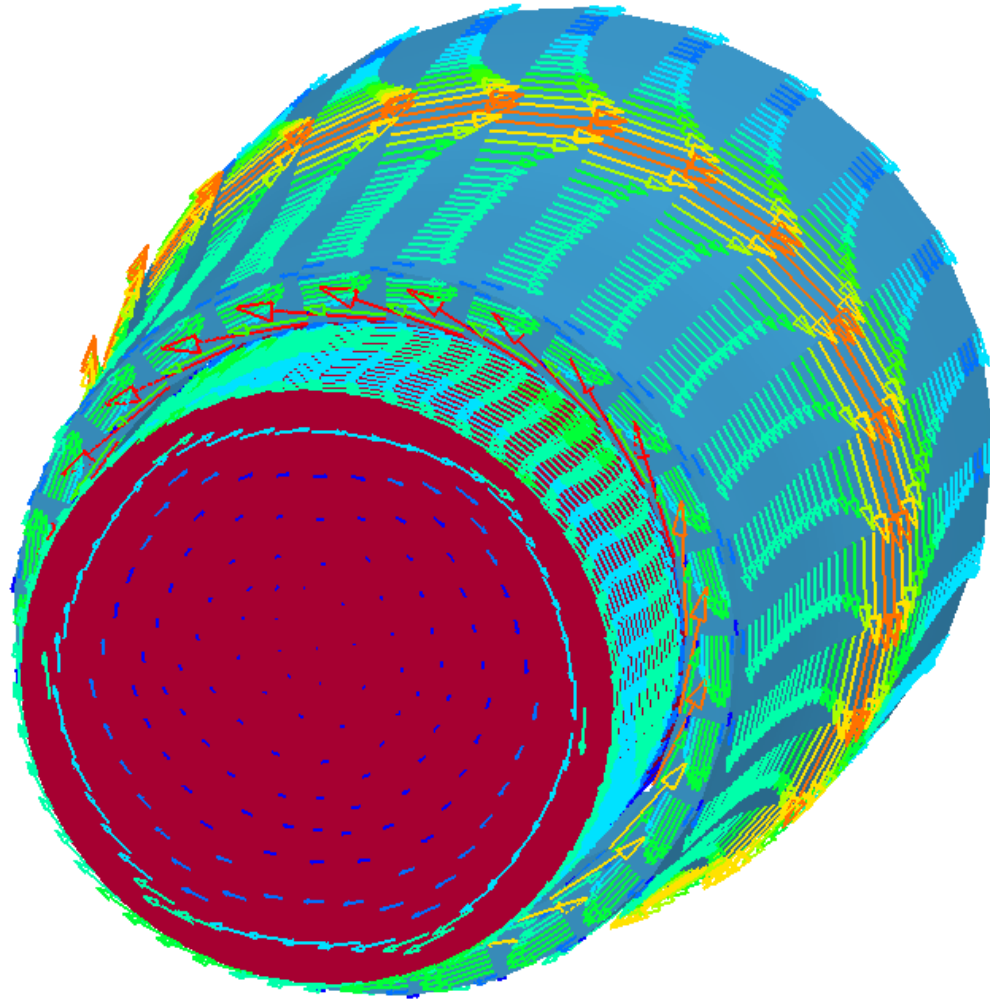


# direction of force without the solid rod, in a tube only model

LS-DYNA keyword deck by LS-PrePost  
Time = 0  
Contours of Effective Stress (v-m)  
min=0, at elem# 251  
max=0, at elem# 251  
Vector of Lorentz force: EM solid integ.  $\sigma_{ij}$   
min=0, at node# 837  
max=0, at node# 837

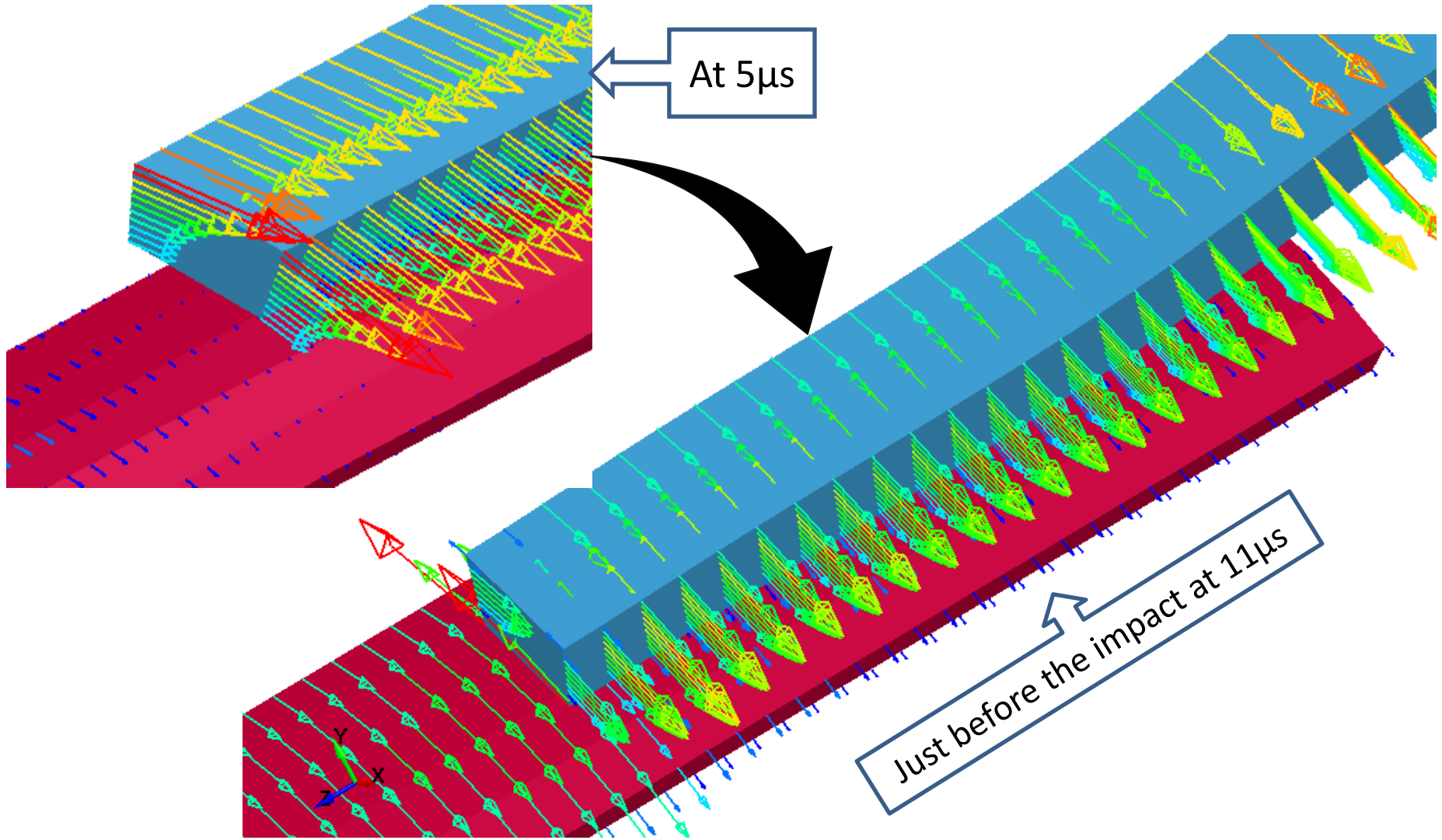


# Eddy current changes in welding model, just Before the impact at $11\mu\text{s}$

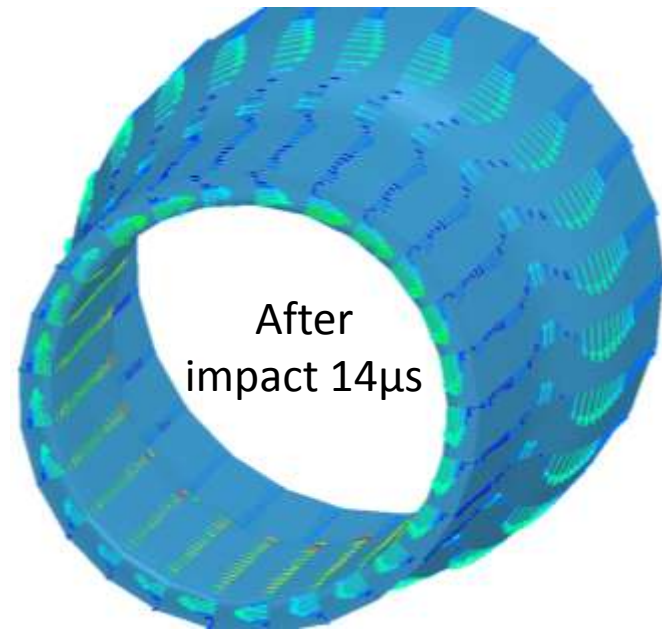
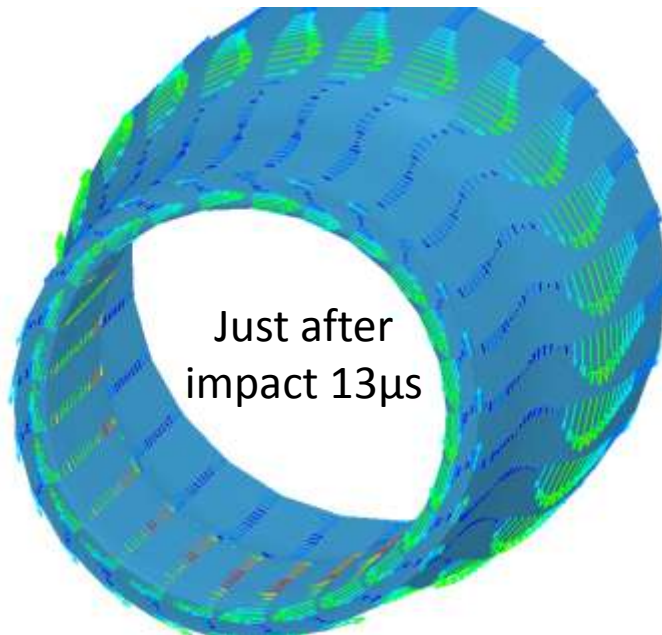
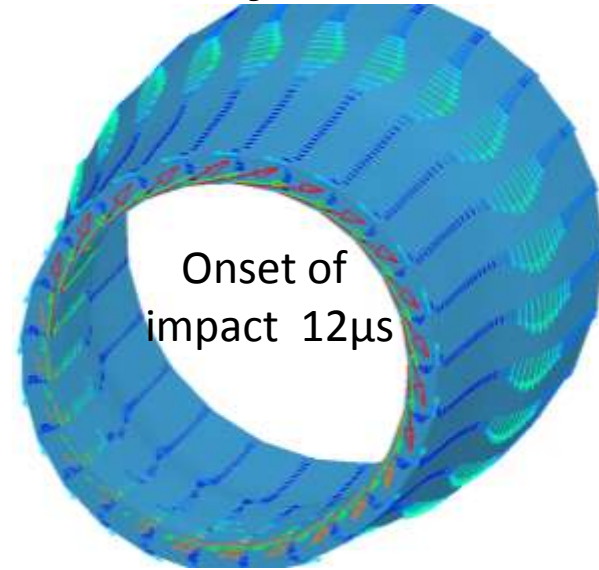
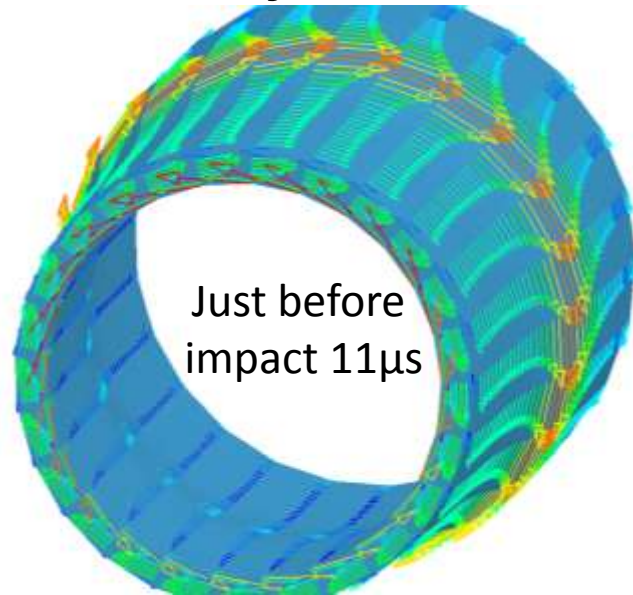




# Eddy current changes in welding model, at $5\mu\text{s}$ and just before the impact at $11\mu\text{s}$



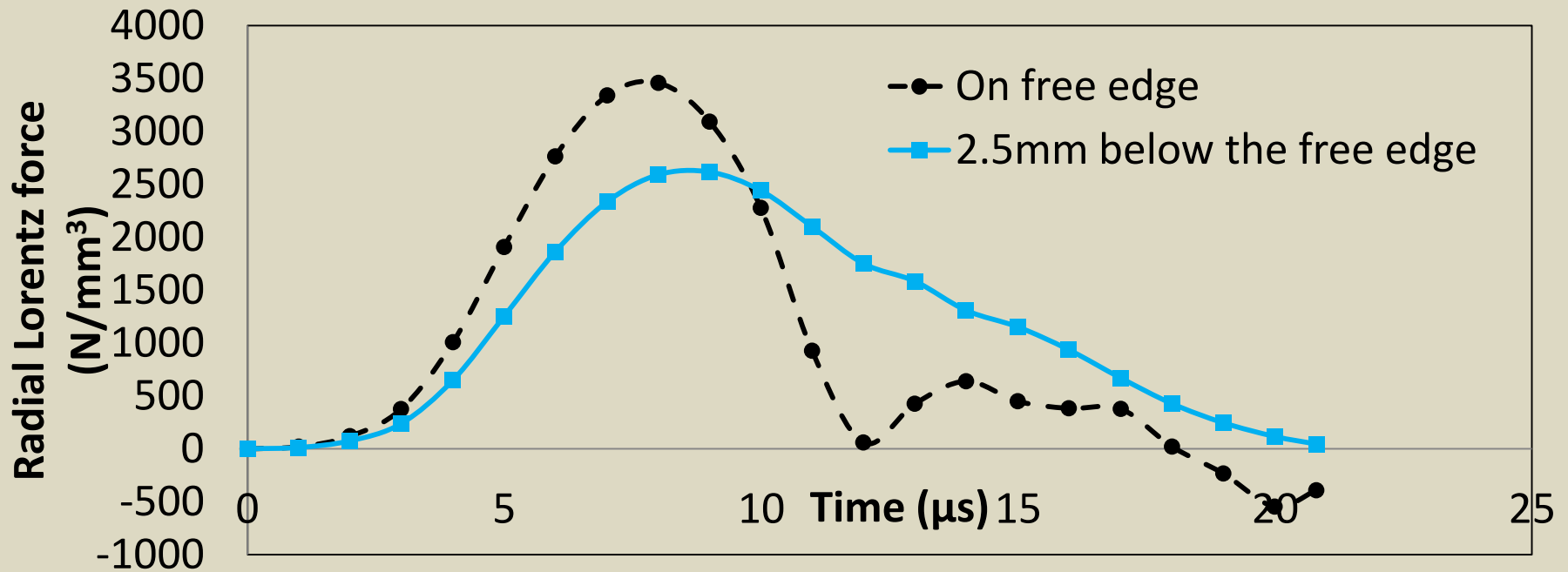
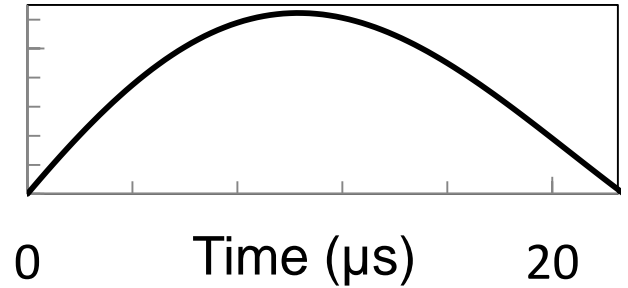
# Eddy current changes in flyer tube



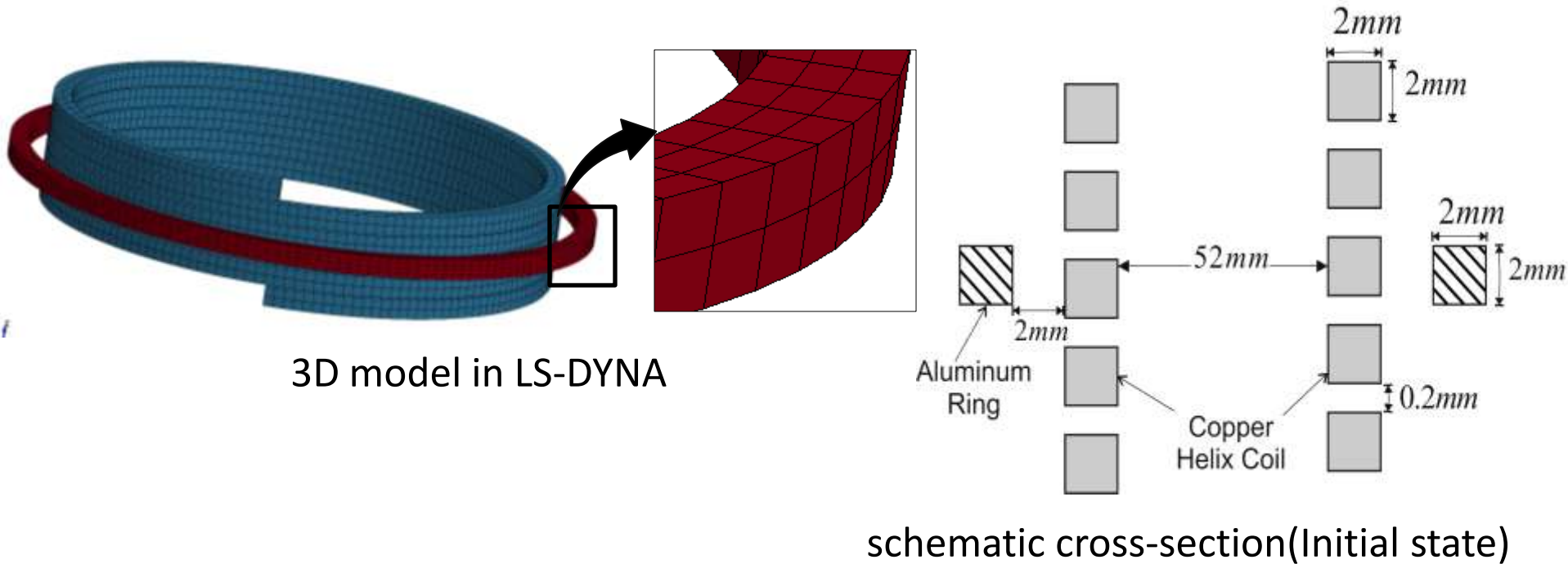
# Average radial Lorentz force near free edge and 2.5mm below the free edge

Source Current

Current  $i$  (kA)



# Ring expansion simulation test

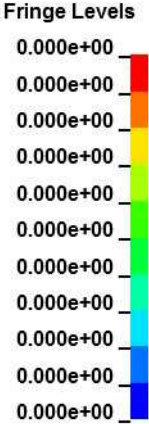
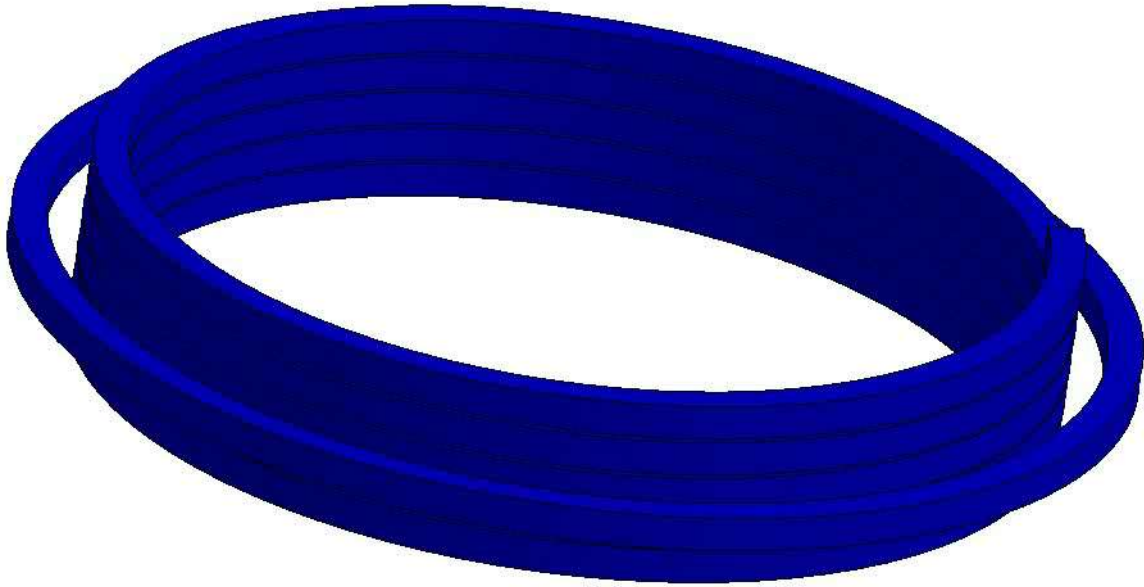


Johnson-Cook parameters used for ring (AA6061-T6)

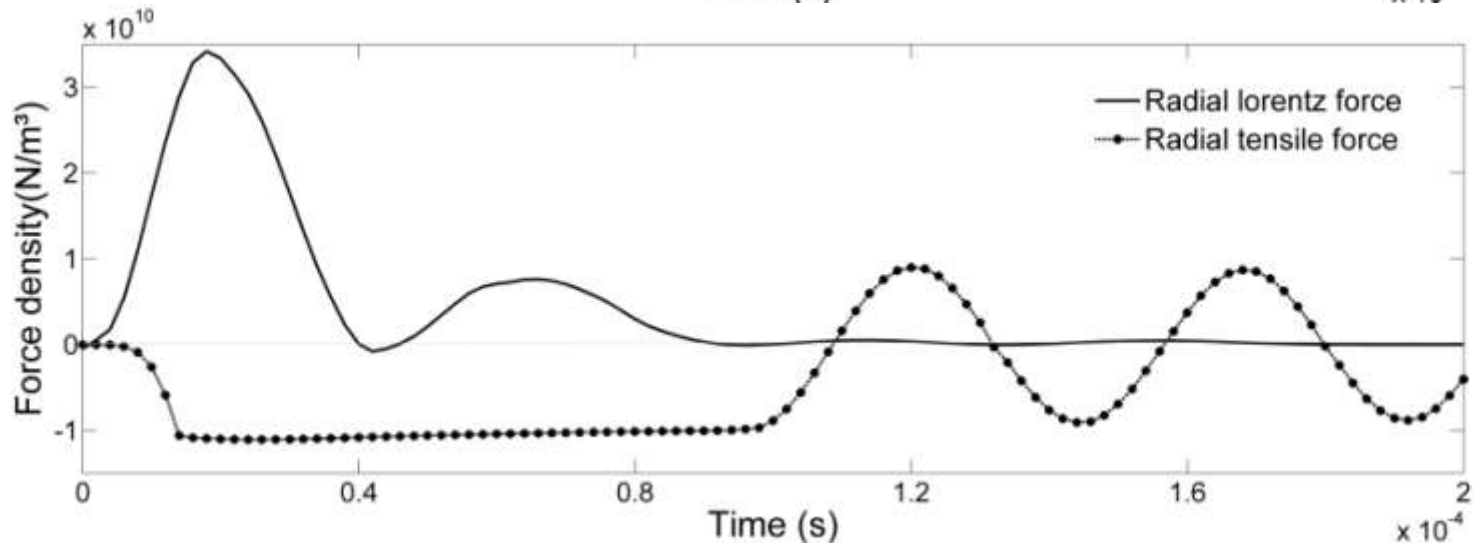
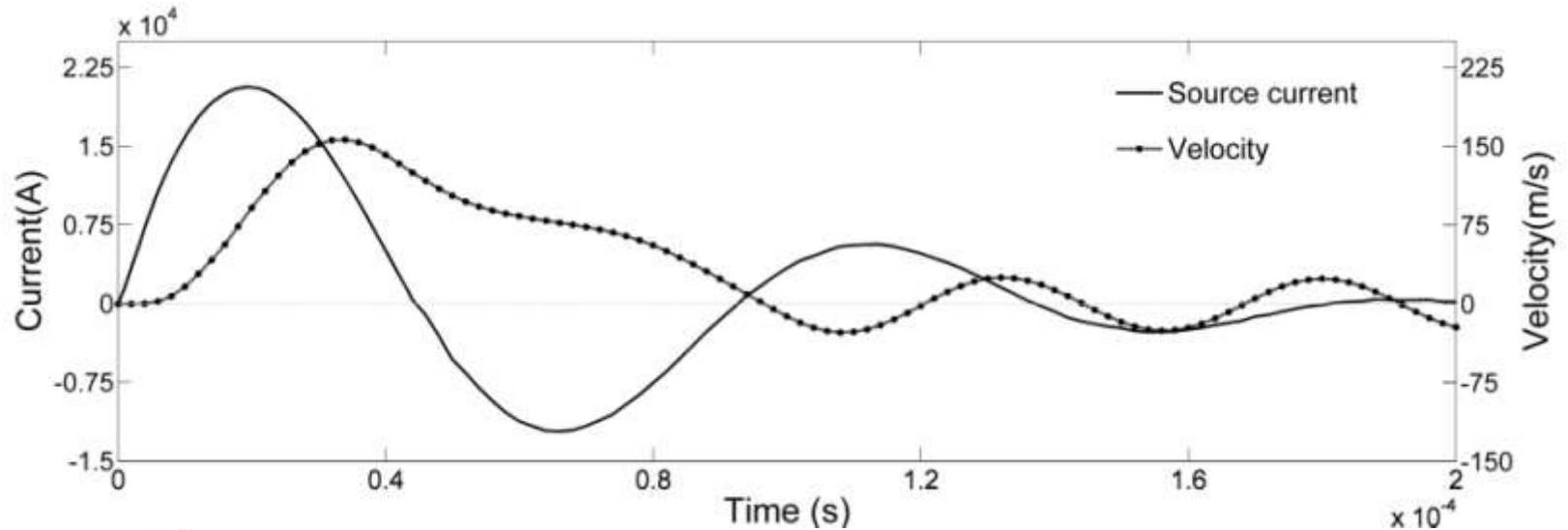
| A (MPa) | B (MPa) | C    | n     |
|---------|---------|------|-------|
| 324     | 114     | 0.42 | 0.002 |

# Plastic strain in the ring expansion

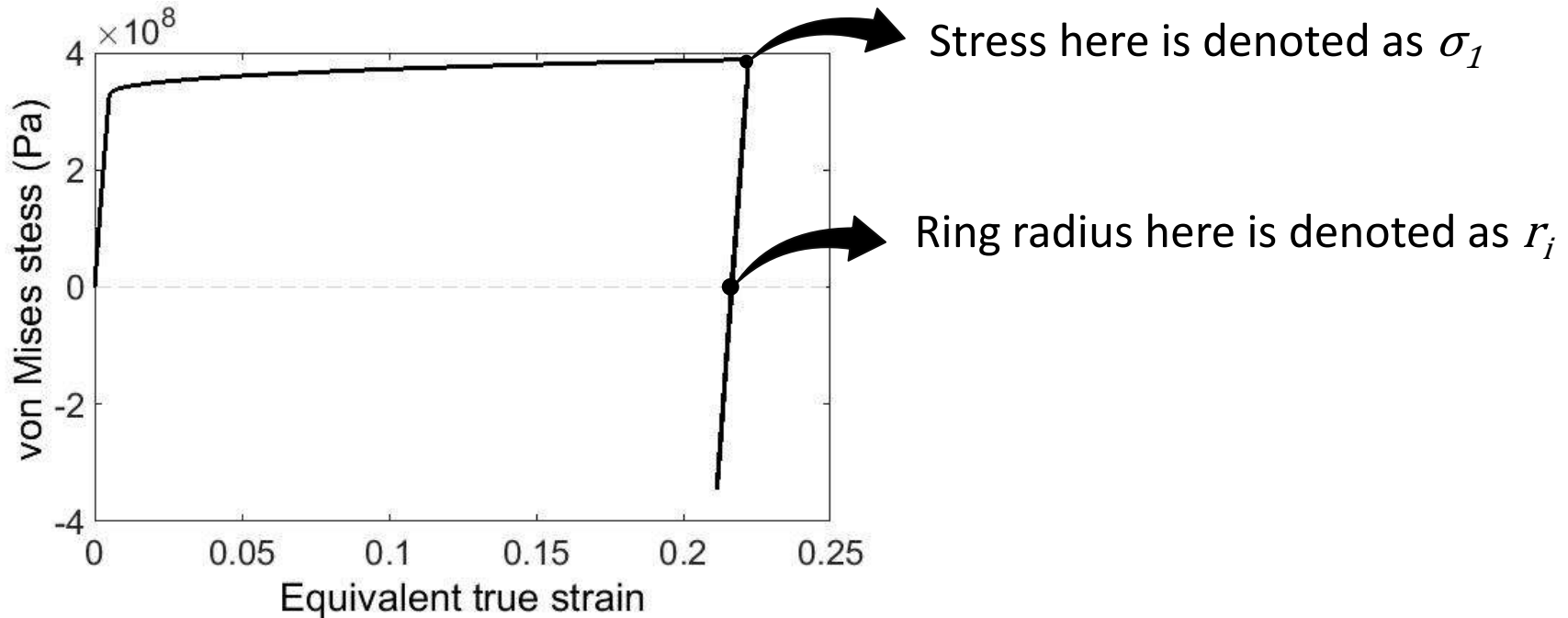
LS-DYNA keyword deck by LS-PrePost  
Time = 0  
Contours of Effective Plastic Strain  
min=0, at elem# 301  
max=0, at elem# 301



# Analysis of process parameters



# Spring back effect



Max spring back radius:

$$\Delta r \approx \frac{\sigma_1}{E} r_i$$

Vibration frequency:

$$f \approx \frac{1}{2\pi r_i} \sqrt{\frac{E}{\rho}}$$

Max spring back velocity:

$$v_{max} \approx \frac{\sigma_1}{\sqrt{\rho E}}$$

# Identification of suitable material models for MPF/MPW

Viscoplasticity:

$$\sigma = \sigma_s \cdot f(\dot{\epsilon})$$

- $\sigma_s$  is the von Mises stress in quasi-static deformations. It could be determined by quasi-static tensile test;
- $f(\dot{\epsilon})$  is the viscoplasticity factor. Two most common models:

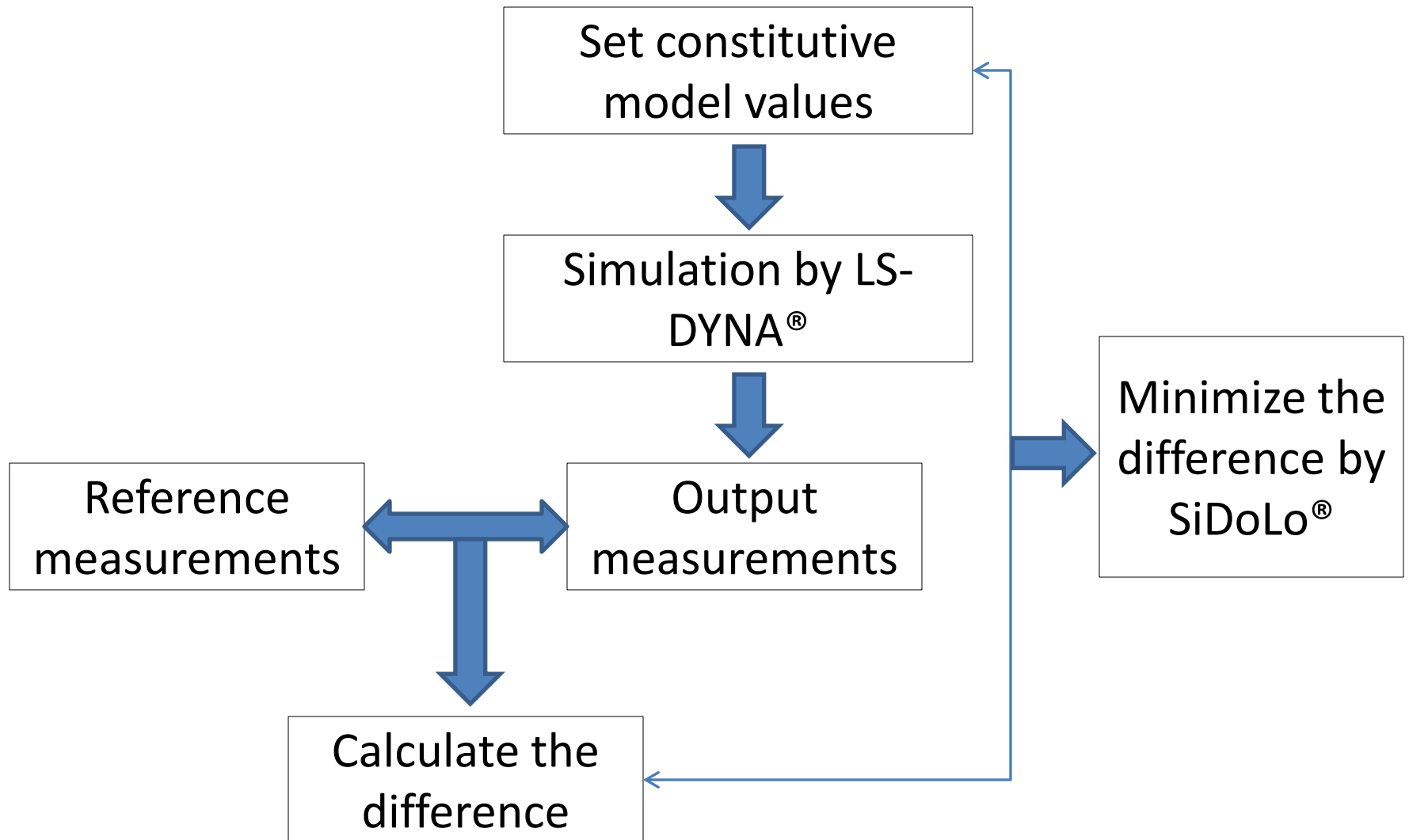
a) Johnson-Cook model:  $f(\dot{\epsilon}) = 1 + C \ln \dot{\epsilon}$

b) Cowper-Symonds model:  $f(\dot{\epsilon}) = 1 + \left(\frac{\dot{\epsilon}}{C}\right)^{\frac{1}{p}}$

[MPF/MPW: Magnetic Pulse Forming / Magnetic Pulse Welding]



# Diagram of identification steps



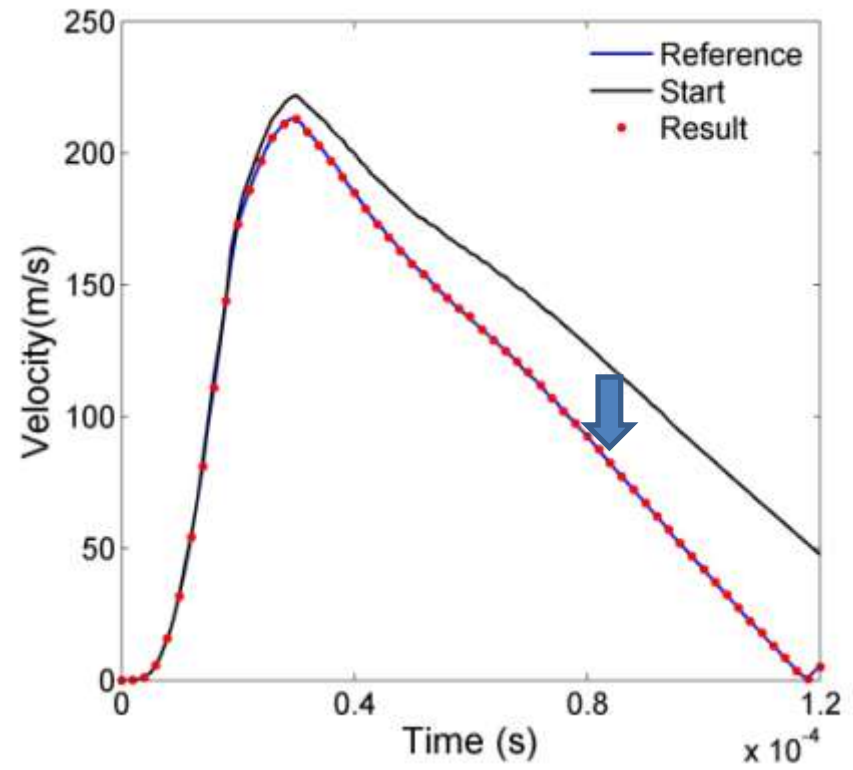
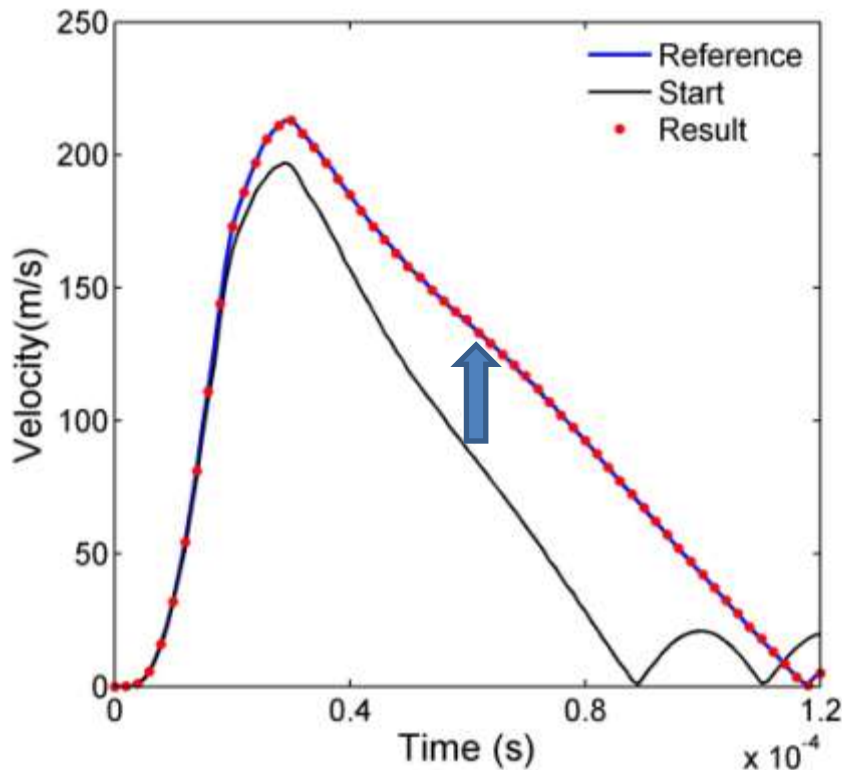
[SiDoLo®: Software toolbox used for identification]

# Result for Johnson-Cook model

Determination of C, with  $\sigma_s = (170 + 423\varepsilon^{0.42})\text{MPa}$

| Target | Start | Result   |
|--------|-------|----------|
| 0.0335 | 0.09  | 0.033503 |

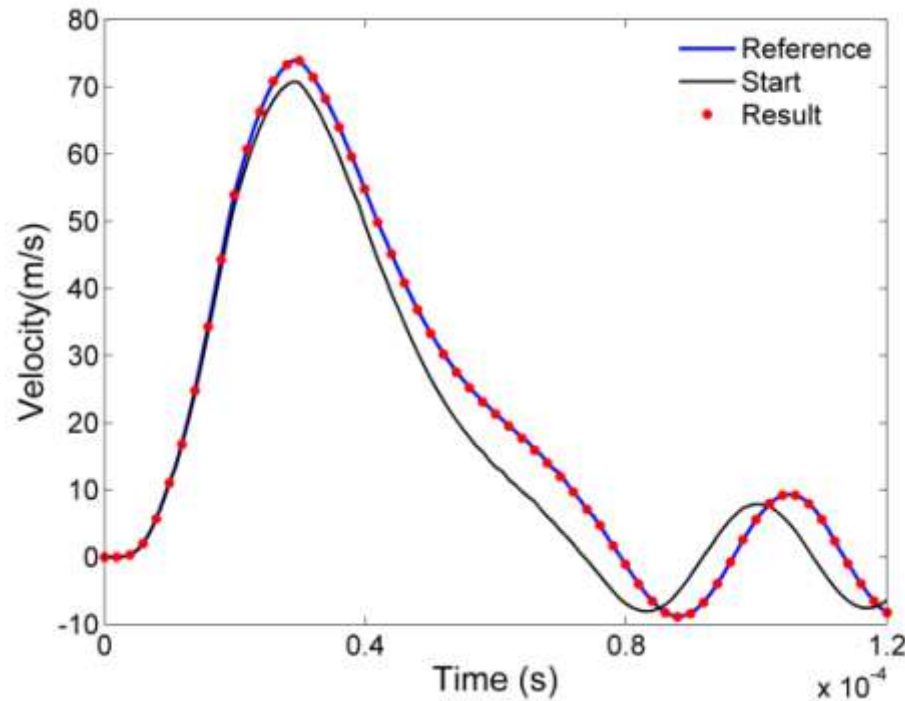
| Target | Start | Result   |
|--------|-------|----------|
| 0.0335 | 0.005 | 0.033383 |



# Result for Cowper-Symonds model

Determination of C and p, with  $\sigma_s = (170 + 423\varepsilon^1)\text{MPa}$

|   | Target | Start | Result  |
|---|--------|-------|---------|
| C | 20000  | 10000 | 19778.6 |
| p | 4.0    | 5.0   | 4.0     |



# Conclusions

- Predictive numerical models were developed for MPF/MPW
- The changes in the deformation behaviours with additional components were investigated
- Fieldshaper slot effect was investigated
- Change in Lorentz force direction and eddy current were also studied
- Changes in electromagnetic field significantly influence the deformation behaviours
- Vibration due to spring back was studied in a ring expansion test
- Numerical models developed for the purpose of identification of material's constitutive models in MPF/MPW

[MPF/MPW: Magnetic Pulse Forming / Magnetic Pulse Welding]

# Thank you for your attention

Authors would like to thank the “Région Picardie” and “Le Fonds européen de développement régional (FEDER)” for their financial support and “Plateforme Innovaltech” for assisting in the development of the numerical model

# Insight into the realistic behaviours of magnetic pulse forming and welding processes using numerical simulations

---



**Questions!**

Insight into the realistic behaviours of magnetic pulse forming and welding processes using numerical simulations

---

**Thank you!**